Improvement of Subsonic Basic Research Tunnel Flow Quality as Applied to Wall Mounted Testing

Brian M. Howerton
Greg Gatlin, Mentor
Research and Technology Group
Applied Aerodynamics Division
Subsonic Aerodynamics Branch

Abstract

A survey to determine the characteristics of a boundary layer that forms on the wall of the Subsonic Basic Research Tunnel has been performed. Early results showed significant differences in the velocity profiles as measured spanwise across the wall. An investigation of the flow in the upstream contraction revealed the presence of a separation bubble at the beginning of the contraction which caused much of the observed unsteadiness. Vortex generators were successfully applied to the contraction inlet to alleviate the separation. A final survey of the wall boundary layer revealed variations in the displacement and momentum thicknesses to be less than $\pm 5\%$ for all but the most upper portion of the wall. The flow quality was deemed adequate to continue the planned follow-on tests to help develop the semi-span test technique.

Nomenclature

δ = boundary layer height, in.

δ^* = boundary layer displacement thickness, in.

θ = boundary layer momentum thickness, in

R_e = Reynolds' number

Q = tunnel dynamic pressure, psf

U_e = local velocity, ft/s

U_i = freestream velocity, ft/s

U_e / U_i = velocity ratio

Background

For subsonic wind tunnel testing, it is desirable to test at as high a Reynolds' number (R_e) as possible in order to make the results closely simulate that which would be obtained at full scale flight conditions. All current tunnels are limited to a maximum R_e as defined by the test conditions and tunnel size. One conceptually simple idea by which to increase the maximum achievable R_e of a facility is to wall mount half of a symmetric configuration allowing it to be made twice as large, thus doubling the test R_e. The problem with such a technique stems from the presence of the wall boundary layer which would submit the submerged portion of the model to velocity gradients not present in real world conditions. Standard practice is to use a platform (or standoff), shaped to match the fuselage at the symmetry plane, to raise the model up out of the wall boundary layer. Unfortunately, most simple standoff shapes generate an adverse pressure gradient of sufficient strength to cause the boundary layer to separate which rolls up to form a horseshoe vortex. It is hoped that certain variations in the standoff geometry might reduce the strength of the horseshoe vortex or eliminate it completely.

316

In order to investigate this phenomenon, a series of tests are to be performed in the Subsonic Basic Research Tunnel (SBRT) to determine the most effective methods of alleviating the horse-shoe vortex. To that end, information is needed concerning tunnel flow characteristics near the wall; specifically the characteristics of the wall boundary layer and the uniformity of that layer across the wall.

Methodology

To ascertain the relevant information about the boundary layer in SBRT, pressure rakes were used to determine the total pressure profiles in the boundary layer of one of the tunnel walls. From this data, velocity profiles were calculated and integrated to determine values of δ, δ^* and θ at each rake location. By varying the rake location vertically along the wall, spanwise changes to these parameters could be discerned. The goal was that these parameters deviate only $\pm5\%$ across the wall surface. It was decided that profiles were to be taken every 1 in. spanwise across the wall to generate a complete picture of the variation of the boundary layer. The original placement of the rakes had one located along the centerline of the wall with another two rakes placed 8 in. above and below the center rake. Each of these were mounted 1.5 in. downstream of the beginning of the test section (station 1). This arrangement was varied until all 17 spanwise locations had been surveyed. The process was then repeated for the case where the rakes were located 27.5 in downstream from the beginning of the test section (station 2) to determine the streamwise variation of the wall boundary layer. For both longitudinal stations, repeat runs were made for each rake location and the results averaged after the data reduction.

Facility and Test Equipment

SBRT is an open circuit, atmospheric wind tunnel having a rectangular test section 22.5 in. wide,32.25 in. high, and 73 in. in length with other pertinent dimensions as shown in Figure 1. The tunnel can be operated up to a maximum Q of 50 psf corresponding to a R_e of 1.31×10^6/ft (U_i=205 ft/s). For this investigation, Q was limited to 20 psf giving a R_e of 8.4×10^5/ft (U_i=132 ft/s). As can be seen from the tunnel diagram, the contraction of this facility is unusually long and gradual with an overall contraction ratio of 6. Its design represents the thinking of early tunnel designers who thought it best to do most of the contracting early followed by a long run of continually lessening curvature.

Prior to testing, some necessary maintenance was performed on the tunnel. The turbulence screens located between the inlet and the contraction entrance were cleaned in order to remove any particulates that could affect the flow. A traversing rig attached to the inlet was removed to reduce the chance of flow separation around its corners and eliminate the unsteadiness that such a separation would cause. Because the tunnel test section operates at subatmospheric pressure, the sidewall had to be stiffened to minimize aeroelastic flexure into the test section which would have caused a discontinuity in the interface between the sidewall and the contraction exit. Furthermore, the contraction exit itself was modified to eliminate any wall waviness and construction seams present.

The two side walls of the tunnel are replaceable to allow rapid changes of model and tunnel configuration. For this test, one side wall was instrumented with three total pressure rakes mounted to the wall surface. Two of the rakes have dimensions as shown in Figure 2 with the third having the same port spacing but one fewer port than the other two rakes for a total of 50 ports. Originally, the pressure instrumentation consisted of two Datametrics 0-100 torr barocells connected by a 48 port Scanivalve to the rakes (the top two ports on the lower rake were not instrumented). One barocell was connected to a pitot-static probe to determine tunnel Q while the other read the rake total pressures. Since the barocells are differential rather than absolute, each was referenced to tunnel static pressure as measured by the pitot-static probe. A Fluke Wireless Hydra Data Logger converted the voltages from the barocells into engineering units (psi) and transmitted the results to a personal computer for storage. The data was then downloaded to a workstation for processing by a FORTRAN data reduction code written by the author to calculate U_e/U_i as a function of distance from the wall. A general uncertainty analysis determined that each pressure measurement gave a calculated velocity that was accurate to within $\pm$ 0.2% of reading using this instrumentation.

Because of the fully turbulent nature of the boundary layer in the test section, multiple readings of a rake port at a given test condition would produce differing results. Therefore a number of runs were used to determine a time averaged reading of the rake pressures. Making such measurements with the Scanivalve-barocell system proved to be extremely time consuming. Thus, an Electronically Scanned Pressure (ESP) system was set up to take data for the final boundary layer survey. The system consisted of a 780B pressure calibration unit (PCU) with a 0-6 psi digiquartz as the calibration reference, two 32 port ESP pressure transducer modules of the ±1 psid range, and the controller/computer interface. Data from the interface was logged into a Hewlett-Packard Apollo 9000 series workstation running an ESP program sourced from the Basic Aerodynamics Research Tunnel. The general uncertainty analysis for the setup revealed a tenfold decrease in accuracy (±2% of velocity reading) as compared to the barocell system but gives the ability to take many more, in this case 2000, samples per data point in seconds rather than 10 per hour. This trade-off was deemed acceptable, but accuracy could be improved with the substitution of 10 inH_2O column modules since ESP accuracy is measured as a percentage of range and the narrower range of these devices would yield greater accuracy.

Results

A baseline survey of the boundary layer was performed with the rakes located at station 1 with a rake configuration of one on the wall centerline and the other two located 8 in. above and below the centerline (designate this placement as wide-rake configuration). The velocity profiles generated are shown in Figure 3 and are the result of 10 runs averaged at each data point (as will all subsequent velocity profiles). From this graph, three general observations can be made. The first is that the profile measured is consistent with that of a turbulent boundary layer since the local velocity is about 65% of freestream very near the wall surface. Calculations comparing the results to the "Law of the Wall" for the logarithmic region of the boundary layer support this conclusion. Also, from the top and bottom rake profiles, it can be seen that δ is about 1.1 in. Most significantly, the profile from the middle rake is showing great irregularity in shape compared to the

318

other two rakes. A look at the results from each individual run (Figure 4) show significant amounts of scatter in the mid rake data that was not observed for the other two rakes. It was theorized that the scatter must be caused by some unsteadiness in the flow field, but the mechanism at the heart of the unsteadiness was not yet known. In an attempt to isolate the affected region, the two outer rakes were brought to within 3 in. of the centerline. Another ten run average was taken giving the profiles seen in Figure 5 which shows good agreement between the three rakes near the wall (as did the wide-rake placement), but with a characteristic 'blip' in the curve around 1 in. above the wall indicative of a low momentum region. It was deduced that the problem most affects the upper region of the boundary layer and is influencing at least a 6 in. path along the center of the sidewall.

After discussion with members of the Subsonic Aerodynamics and Flow Modeling and Control branches, it was thought that the flow problems could be due to the tunnel design. Investigation revealed the presence of a three inch straight wall section between the last turbulence screen and the start of the contraction creating a corner that could possibly cause the flow to detach from the wall and form a separation bubble in that region. Previous work has shown that vortex generators (VG's) can be effective in keeping flow attached in wind tunnel diffusers, but the application of them in a wind tunnel contraction is much less common. To test this flow control method, counterrotating vortex generators having a plow-shaped planform were applied to the straight section just upstream of the tunnel contraction along the wall of the tunnel the rakes were mounted. Two sizes were tested with the smaller having a length of 1 in. and a height of 0.5 in. and the larger being 3 in. long by 1 in.in height These generators are commercially available and were originally intended as a drag reduction device for large commercial transport trucks. The generators were spaced such that the smaller had 2 in. between devices with the large VG's were spaced at 3.5 in. intervals.

Figure 7 shows the boundary layer velocity profiles with the small VG's applied. Significant improvement can be seen in the bottom rake profile as evidenced by the lack of the 'bump' in the profile between 0.8 in. and 1.0 in from the wall. The upper and middle rake profiles show slight changes toward a more continuous profile, but significant irregularities still exist. One other point of difference is the height of the boundary layer for the three profiles with the middle and upper being 0.2 in. and 0.5 in. thicker respectively than the lower. Given the positive, albeit small, effect of the small VG's it was thought that the larger version may be more effective in correcting the problem.

Once the large VG's were applied and data was taken, it became obvious that a solution was at hand. From Figure 7, one can see that the data points from each rake are much more coherent for a given height above the wall and that the boundary layer heights are within 0.1 in of each other. The small variations that remain between profiles were thought to be due to the small number of samples taken for each data point and not due to actual flow physics. Thus, confidence was high that the contraction problem had been solved.

One concern that arose about the application of VG's to the tunnel contraction was the effect of the added vorticity on models in the test section created by the VG. Past literature has shown that the vorticity created damps out fairly quickly and can be considered negligible at distances 100 device heights downstream or greater. Since the contraction is over 100 in. in length, it was assumed that the problem would be nonexistent. In order to verify the assumption, as well as to

try and document the existence of the separation bubble in the contraction, flow visualization tufts were placed on the contraction wall and imaged with a video camera to record their movement. With the VG's removed, the tufting was able to reveal the existence of the separation bubble as postulated. Tufts placed in the corner region exhibited a reversal in direction that can be associated with the backflow of the fluid in the corner region. Replacing the VG's eliminated the backflow condition and promoted attached flow throughout the contraction. Also evident was the rapid diminishment of the induced vorticity as one moved downstream of the generators with no visible tuft deflection due to the VG's approximately 2 ft downstream of the devices.

At this point, the full survey began using the ESP system to determine the pressure data. Because the ESP modules are sensitive to temperature variation, care was take to keep room temperature variation during a run to within 2 degrees of room temperature at calibration. A minimum of two runs were made at each of the 17 rake locations at each longitudinal station with each run being the average of 10 data sets of 200 samples per set. Next, the data was reduced to determine the velocity profiles as well as values of δ, δ^*, and θ for each run. These values for each run were averaged to give one set of parameters at a given rake location. Figure 9 shows the result of this survey at both longitudinal stations. From the lowermost rake position until 4 in above the centerline, variations in the momentum and displacement thicknesses fall within $\pm 5\%$ of the average value of these parameters. The upper portion of the wall experienced an increase in both parameters beyond the range deemed acceptable. A possible explanation for this phenomenon is the absence of an entrance lip to the top of the tunnel inlet (due to physical limitations of the room) causing some type of unsteadiness; however, more investigation will be needed to isolate the cause. Fortunately, for the model mounting and angle of attack range planned in the facility, the variation of the boundary layer near the top of the wall will not effect the results.

Conclusions

From this investigation some conclusions may be drawn:

1. Properly sized vortex generators are effective in eliminating some separation problems caused by poor contraction designs.

2. From the standpoint of boundary layer uniformity, SBRT is adequate to test wall mounted models as long as the angle of attack range is such that the model is not placed on the upper part of the wall.

Further work could be done to optimize the spacing and size of the vortex generators to minimize the added vorticity while maintaining attached flow. Also, application of the generators could be extended to the other three sides of the tunnel possibly improving the results along the upper portion of the wall.
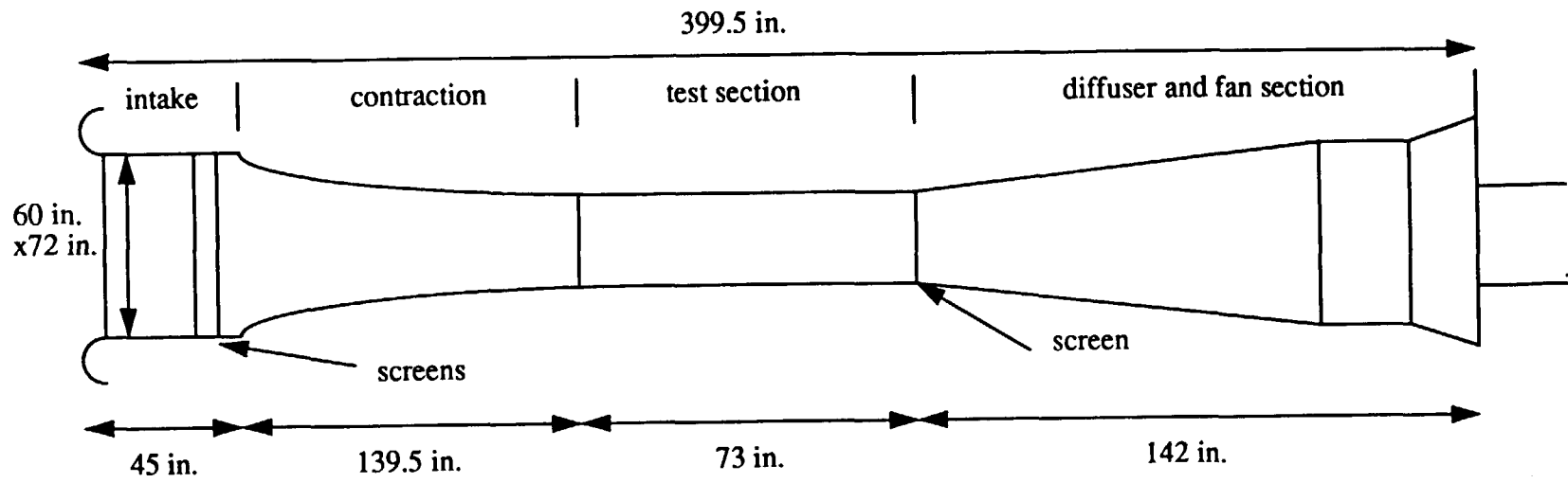
320

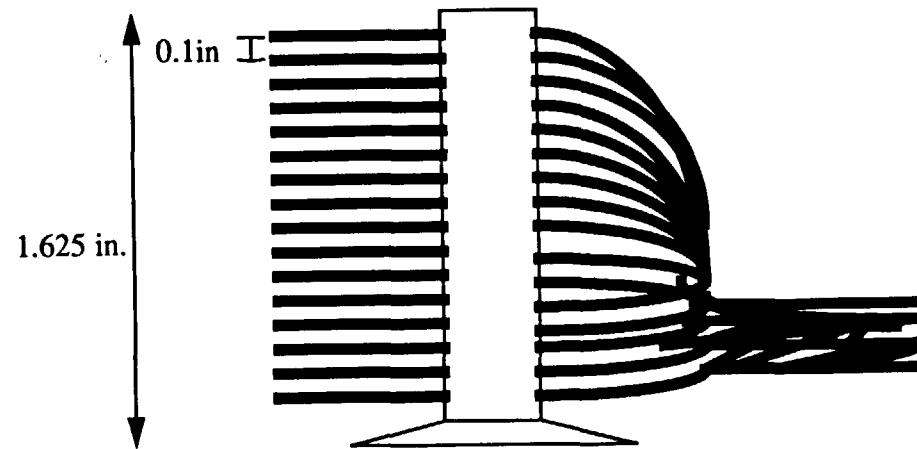Figure 1. Plan layout of SBRT showing relevant dimensions.
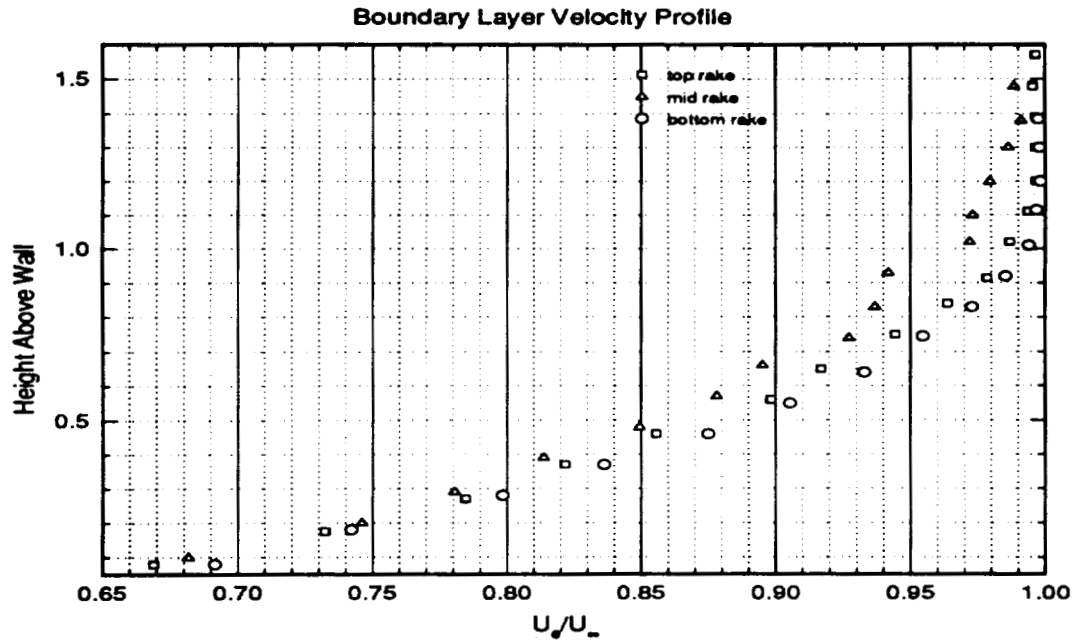

Figure 2. Boundary layer total pressure rake.

Boundary Layer Velocity Profile

Figure 3. Baseline Boundary Layer Survey.

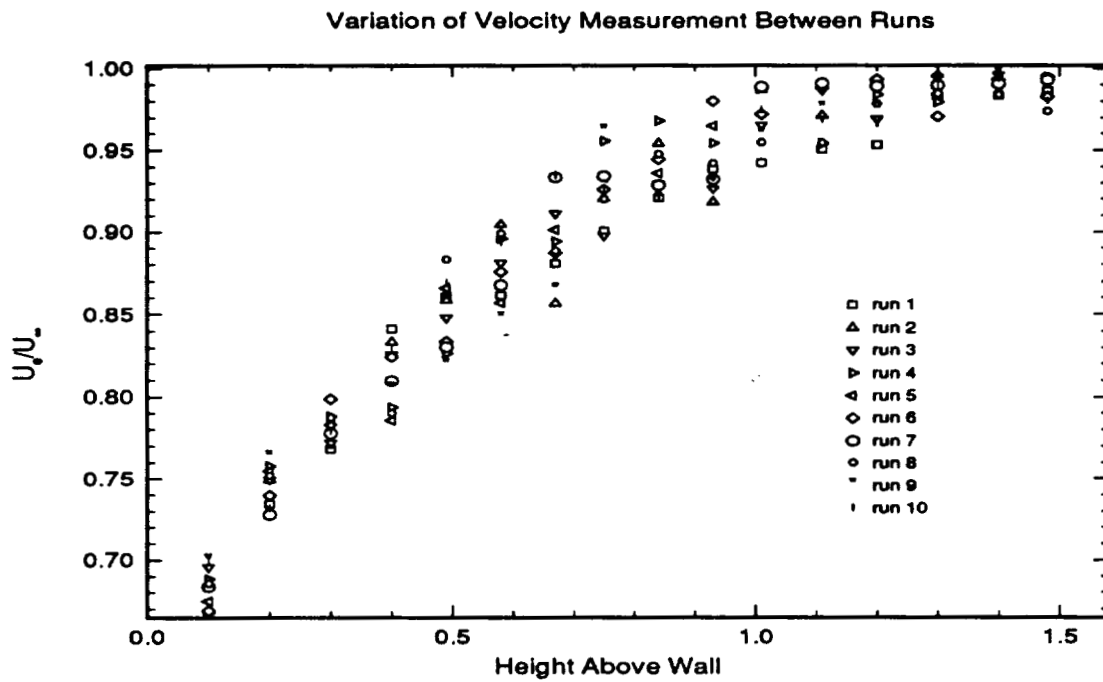**Variation of Velocity Measurement Between Runs**

Figure 4. Scatter of Data Between Runs.
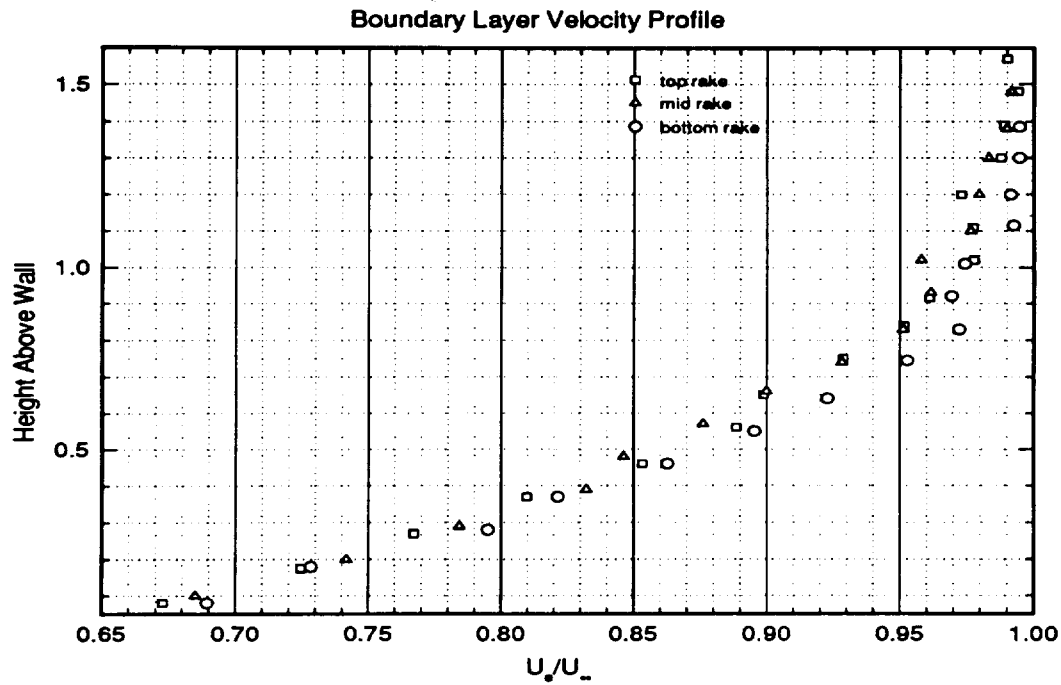
Figure 5. Narrow Rake Placement Baseline Survey.
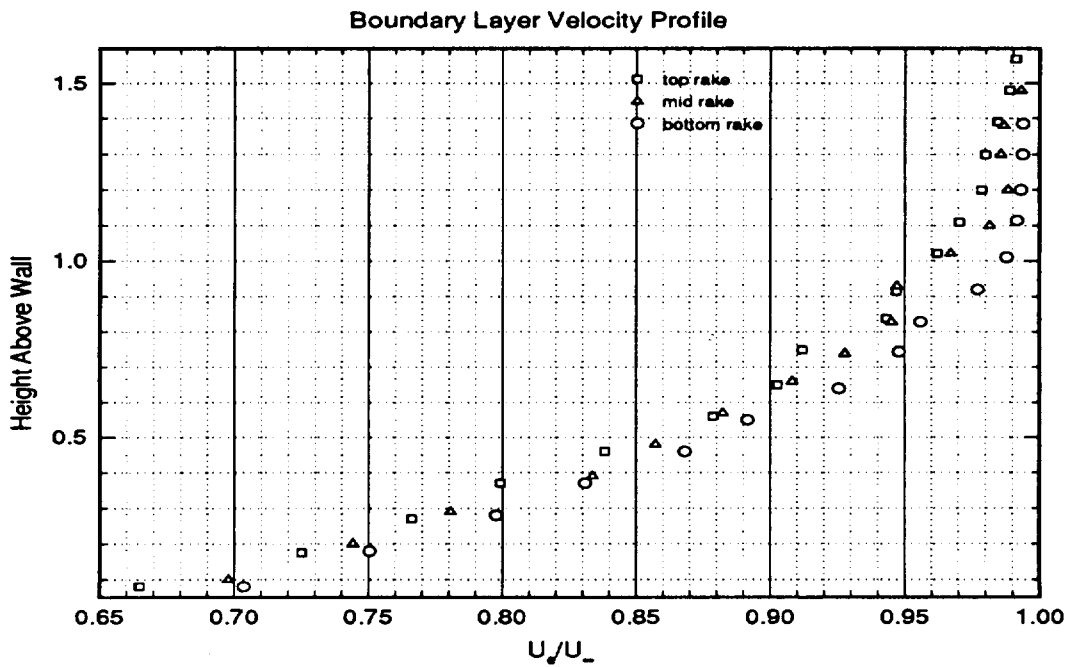
Figure 6. Narrow Rake Placement, Small VG's Applied.
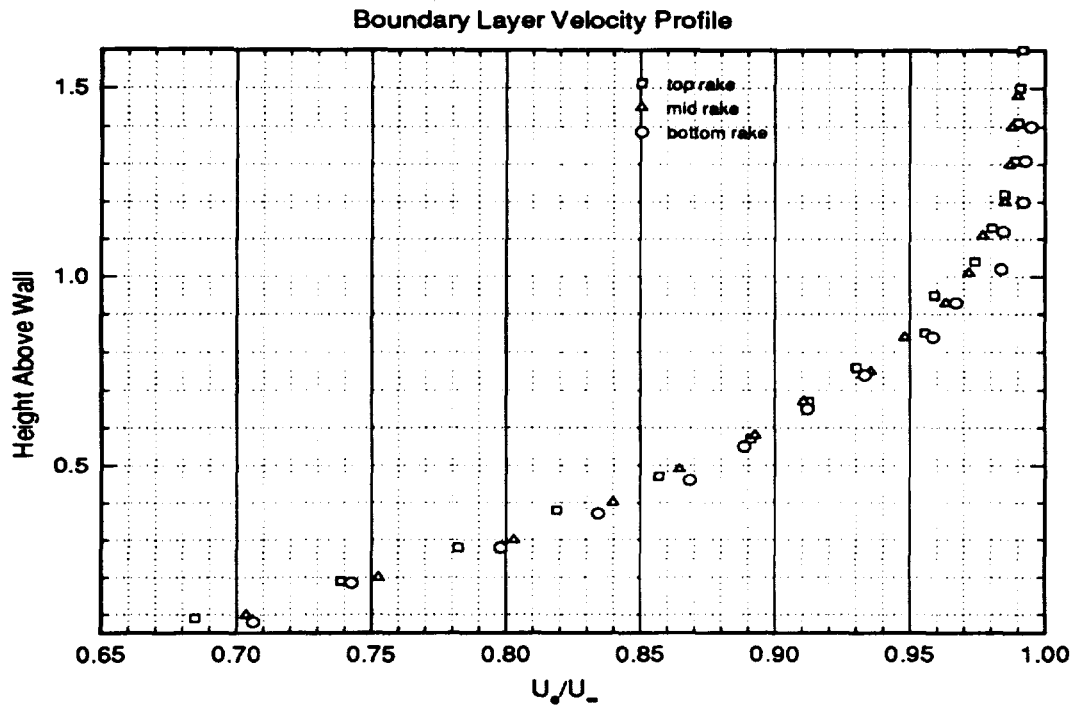
Boundary Layer Velocity Profile

Figure 7. Narrow Rake Placement, Large VG's Applied.

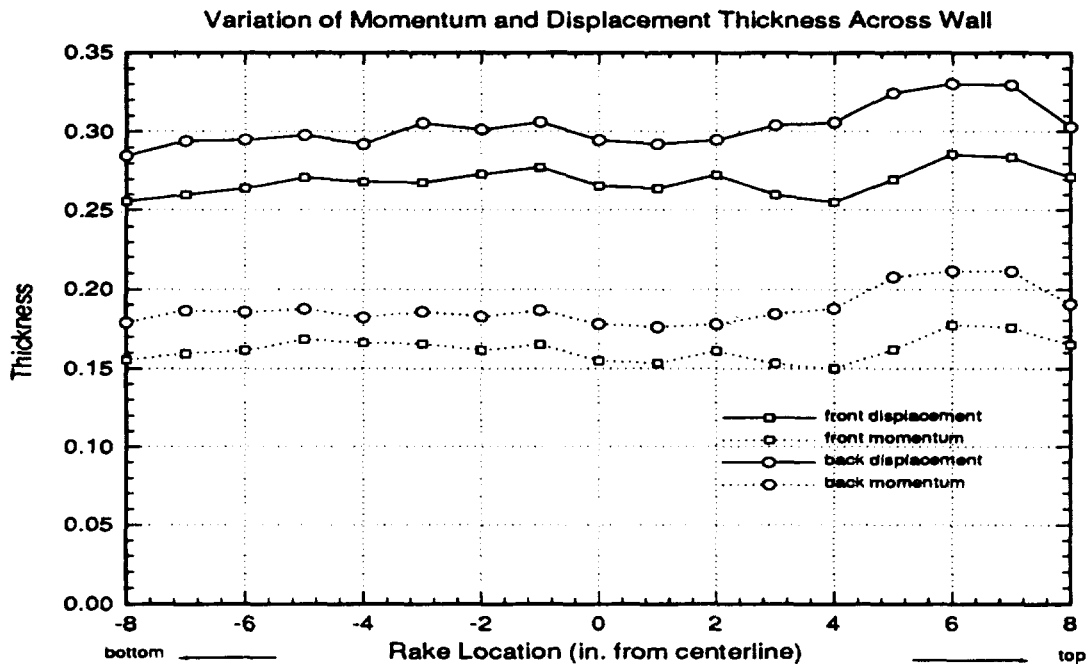**Variation of Momentum and Displacement Thickness Across Wall**

Figure 8. Variation of Boundary Layer Parameters.